

THE ANALYSIS OF THE CONVECTIVE-CONDUCTIVE HEAT TRANSFER IN THE BUILDING CONSTRUCTIONS

Zbynek Svoboda

Czech Technical University in Prague
Faculty of Civil Engineering
166 29 Prague 6 - Czech Republic

ABSTRACT

The numerical model for the analysis of the combined convective-conductive heat transfer in the building components has been developed. Presented model is based on the partial differential equation for the two-dimensional steady-state heat transport caused by conduction and convection. The finite element method was used to obtain the numerical solution of the governing equation. The general finite element formulation was derived by means of the Petrov-Galerkin approach.

The developed computer program was used to study one typical lightweight building wall construction. The results of simulation demonstrate that the lightweight constructions insulated with permeable mineral wool are very sensitive to the convective heat transfer.

INTRODUCTION

The combined heat transfer caused by conduction and convection takes place in building constructions loaded by the temperature and the pressure difference between the interior and the exterior. The importance of the convective-conductive heat transfer depends mainly on the type of the construction and on its tightness against the air flow.

In traditional building constructions with no cracks, the convective component of the heat transfer is negligible in comparison with the prevailing conductive component. On the other hand, modern lightweight constructions with a thermal insulation, which is permeable to the air flow and which is covered with only thin layers of plasterboards and similar materials, are very sensitive to the convective heat transfer.

The analysis of the combined convective-conductive heat transfer could be based on the partial differential equation for the two-dimensional steady-state heat transport in a porous medium. This equation can be expressed as

$$\lambda \nabla^2 T + \rho_a c_a \frac{k}{\mu} \vec{\nabla} p \cdot \vec{\nabla} T = 0 \quad (1).$$

The first term on the left-hand side of the equation (1) represents the heat transport due to conduction, the second term represents the heat transport due to convection. Although it is possible to use all standard boundary conditions for the equation (1), the Newton boundary condition defined as

$$-\lambda \frac{\partial T}{\partial n} + v_n \rho_a c_a (T - \bar{T}) = \alpha (T - \bar{T}) \quad (2)$$

is usually the most useful for the purposes of the building physics analysis.

The numerical solution of the equation (1) with the boundary condition (2) was derived using following assumptions:

- heat transfer is steady-state and two-dimensional
- convection of air through the building construction is caused only by pressure difference
- the air is incompressible,
- flow of air is linear according to Darcy's Law

$$\vec{v} = -\frac{k}{\mu} \vec{\nabla} p \quad (3)$$

- pressure distribution is governed by Laplace equation

$$k \cdot \nabla^2 p = 0 \quad (4)$$

- the radiative heat transfer is not considered in the model directly but only by means of heat transfer coefficient

$$\alpha = \alpha_c + \alpha_r \quad (5)$$

- the pressure losses of cracks are considered in the model in a simplified way by means of „equivalent“ permeability of the air in the crack, which is defined as

$$k_a = \frac{b^2}{3} \quad (6)$$

and which was derived from the equality of the air flow velocity defined by Darcy's Law and the mean velocity of the laminar air flow in the crack defined as

$$\bar{v} = \frac{\Delta P}{\mu L} \frac{b^2}{3} \quad (7).$$

ANALYSIS

The equation (1) is a typical example of the convective-diffusion equation. The search for the numerical solution of the convective-diffusion equation is always more complicated than the search for the solution of the related diffusion equation. The main cause is the convective transport term which can introduce under certain conditions instabilities in the numerical solution.

The finite element method was used to find the solution of the equation (1). The general finite element formulation was derived by means of the Petrov-Galerkin process. As the Petrov-Galerkin process is one of the weighted residuals methods, the derivation of the finite element formulation starts with equation

$$\int_{\Omega^{(e)}} \left[\lambda \nabla^2 T + \rho_a c_a \frac{k}{\mu} \vec{\nabla} p \vec{\nabla} T \right] W_i d\Omega = 0 \quad (8).$$

The equation (8) is a mathematical expression of the requirement that the residual of the numerical solution of the equation (1) must be orthogonal to the weighting functions W_i .

The unknown function T in equation (8) is taken as approximation

$$T = N_i^T T_i \quad (9).$$

The interpolation functions N_i are known functions closely connected to the type of the chosen finite elements.

The definition of the weighting functions W_i is very important in this case. The approach recommended by Zienkiewicz takes the weighting functions as

$$W_i = N_i + \varepsilon \frac{h}{2} \frac{u \frac{\partial N_i}{\partial x} + v \frac{\partial N_i}{\partial y}}{|u|} \quad (10).$$

Now, if the value of ε is chosen as

$$\varepsilon = \coth Pe - \frac{1}{Pe} \quad (11)$$

and Peclet number as

$$Pe = \frac{\rho_a c_a |u| h}{2\lambda} \quad (12)$$

then according to Zienkiewicz the numerical oscillations do not arise for any possible rate between convective and conductive heat transport.

The general finite element formulation can be finally derived from the equation (8) by means of integration by parts and by means of introduction of the boundary condition (2) and written as

$$(K_\lambda + K_v + K_\alpha) T_i = q_\alpha \quad (13).$$

The conductance matrix K_λ is defined as

$$K_\lambda = \int_{\Omega^{(e)}} \lambda \left(\frac{\partial W_i}{\partial x} \frac{\partial N_i^T}{\partial x} + \frac{\partial W_i}{\partial y} \frac{\partial N_i^T}{\partial y} \right) d\Omega,$$

the convective transport matrix K_v as

$$K_v = \int_{\Omega^{(e)}} \rho_a c_a \left(u W_i \frac{\partial N_i^T}{\partial x} + v W_i \frac{\partial N_i^T}{\partial y} \right) d\Omega,$$

the boundary conditions matrix K_α as

$$K_\alpha = \int_{\Gamma^{(e)}} (\alpha - v_n \rho_a c_a) W_i N_i^T d\Gamma$$

and the boundary conditions vector q_α as

$$q_\alpha = \int_{\Gamma^{(e)}} (\alpha - v_n \rho_a c_a) W_i \bar{T} d\Gamma.$$

Note that the convective transport matrix K_v is asymmetrical, which leads to the asymmetrical matrix of the linear equations system for unknown nodal values T_i .

The computer model „WIND“ developed by Z. Svoboda is based on the equation (13). It calculates the pressure field within the porous building construction, the air flow velocity field, the temperature field and the heat flow rate due to conduction and due to convection.

The analysis of the numerical stability of the solution obtained by the computer program „WIND“ was realised in two ways. The first method was based on the comparison of the numerical solution with the exact analytical solution of the equation

$$\lambda \frac{d^2 T}{dx^2} - \rho_a c_a u \frac{dT}{dx} = 0 \quad (14)$$

with boundary conditions

$$T(0) = 1, \quad T(1) = 0 \quad (15).$$

The analytical solution of the equation (14) is

$$T(x) = \frac{e^{Ax} - e^A}{1 - e^A} \quad (16)$$

with the value of A defined as

$$A = \frac{\rho_a c_a u}{\lambda} \quad (17).$$

The numerical solution of the equation (14) for the value of $A=4$ and for various number of the finite elements in comparison with the exact solution could be seen in Table 1. The analysis shows clearly that the results of the numerical solution converge to the exact solution with increasing number of the finite elements covering the solved area.

Table 1 Results of the exact and the numerical solution

Distance	Temperature			
	exact solution	numerical solution		
x [m]	T [K]	T ₁ [K]	T ₂ [K]	T ₃ [K]
0,0	1,000	1,000	1,000	1,000
0,2	0,977	0,978	0,977	0,977
0,4	0,926	0,928	0,927	0,926
0,6	0,813	0,815	0,814	0,813
0,8	0,561	0,564	0,562	0,561
1,0	0,000	0,000	0,000	0,000
Number of elements	---	20	40	80

The second method of the numerical stability analysis was based on the evaluation of the functional corresponding to the equation (1). The finite element method is one of the variation methods which means that the exact solution of the equation (1) obtained by the finite element method must minimise the functional corresponding to the equation (1). The functional connected with the equation (1) could be derived by means of the Guymon's process cited by Zienkiewicz in the following form

$$F = -\frac{1}{2} \int_{\Omega} q \lambda \left[\left(\frac{\partial T}{\partial x} \right)^2 + \left(\frac{\partial T}{\partial y} \right)^2 \right] d\Omega \quad (18)$$

$$- \int_{\Gamma} q (\alpha - \nu_n \rho_a c_a) \left(\frac{1}{2} T^2 - T \bar{T} \right) d\Gamma$$

where the value of q is defined as

$$q = e^{-\frac{\rho_a c_a}{\lambda}(ux+vy)} \quad (19).$$

The building construction shown on Fig. 1 was chosen to be analysed from the point of view of the numerical stability of the calculation results. The boundary conditions were taken as follows:

- interior: temperature 20 °C, pressure 0 Pa
- exterior: temperature -15 °C, pressure 10 Pa

The initial mesh system with 580 finite elements is shown on Fig. 2. The mesh system was refined twice and each time the functional (18) was calculated by means of the Gauss numerical integration. The results of the analysis are presented on Fig. 3. It could be clearly seen that the values of the functional decrease with the increasing number of finite elements. This shows that the calculated results of the equation (1) converge to the exact solution and the numerical stability is reached.

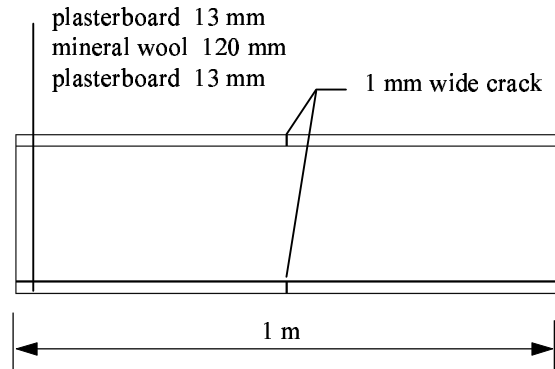


Fig. 1 The analysed building construction

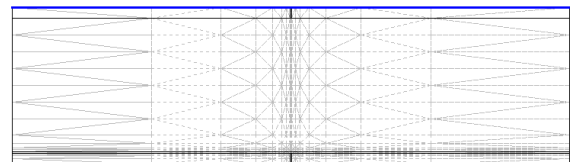


Fig. 2 The initial mesh system with 580 elements

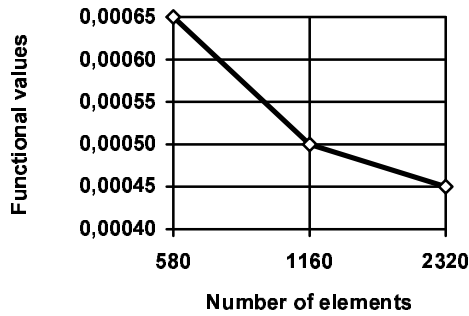


Fig. 3 The calculated functional values

SIMULATION

The typical lightweight building wall construction has been chosen to be the object of simulation. The analysed construction, which is shown on Fig. 1, consists of two plasterboards attached to the wood frame. The space between the plasterboards is filled with the thermal insulation from the mineral wool. The material characteristics used in the following analysis are described in Table 2.

The calculation has been performed several times:

- for the tight construction with no cracks
- for the construction with only one crack in the plasterboard on one side of the mineral wool
- for the construction with two cracks in various distances in the plasterboards on both sides of the mineral wool.

Table 2 Used material characteristics

Material	Permeability [m ²]	Thermal conductivity [W.m ⁻¹ .K ⁻¹]
plaster-board	1.10 ⁻¹²	0,220
mineral wool	1.10 ⁻⁹	0,040

The width of the crack has been chosen as 1 mm. The pressure difference loading the construction has been taken as 10 Pa and the temperature difference as 35 °C (the same values as in the case of the previously described numerical stability analysis).

The influence of the convective heat transport through the crack has been expressed for each analysed construction by means of the convective linear thermal transmittance according to the following equation

$$\psi_{v,\Delta p} = \frac{\Phi}{t_i - t_e} - U \cdot l \quad (20).$$

The linear thermal transmittance is used in ISO and European standards as a value showing the influence of a thermal bridge on the heat loss. In this paper, the crack is taken as a „convective bridge“ and the convective linear thermal transmittance is used to show the influence of the air flow through the „convective bridge“ on the heat loss, which can be finally expressed as

$$Q = \sum A \cdot U \cdot \Delta t + \sum l_v \cdot \psi_{v,\Delta p} \cdot \Delta t \quad (21).$$

The convective linear thermal transmittance is always related to the length of the crack and to the operating pressure difference.

The results of the convective linear thermal transmittance calculation for the pressure difference of 10 Pa are shown in Table 3 and on Fig. 4.

Table 3 The results of calculation

Description	Convective linear thermal transmittance $\Psi_{v,10 Pa}$ [W.m ⁻¹ .K ⁻¹]	Air flow into the interior V [m ³ .s ⁻¹ .m ⁻²]
no crack	0,009	2,9.10 ⁻⁵
crack on one side of the construction only	0,017	5,4.10 ⁻⁵
cracks on both sides of the construction:		
• opposite each other and in distance of:	0,367	20,9.10 ⁻⁵
• 50 mm	0,342	20,8.10 ⁻⁵
• 100 mm	0,249	19,8.10 ⁻⁵
• 200 mm	0,174	19,0.10 ⁻⁵
• 500 mm	0,094	15,0.10 ⁻⁵

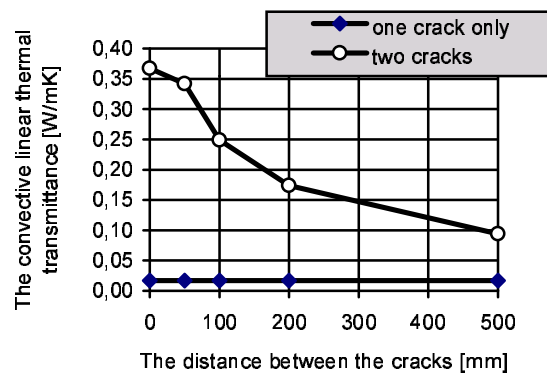
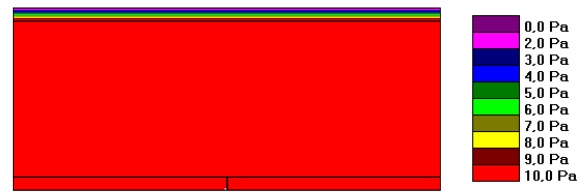


Fig. 4 The convective linear thermal transmittance for the difference of 10 Pa

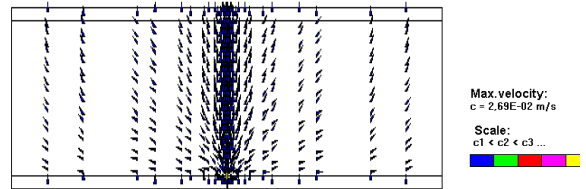
The pressure fields, the air flow velocity fields and the temperature fields for the tight construction, for the construction with the crack on one side of the mineral wool and for the construction with the cracks in both plasterboards are presented on Fig. 5, Fig. 6, Fig. 7 and Fig. 8.

Note the deformations of the temperature fields which are in the cases of untight constructions caused by the air flow through the cracks in mineral wool coverings. Such temperature deformation is visible even in the case of the construction with the crack in only one plasterboard (Fig. 6) and reaches very extensive level in the case of the construction with the opposite cracks in both coverings (Fig. 7).

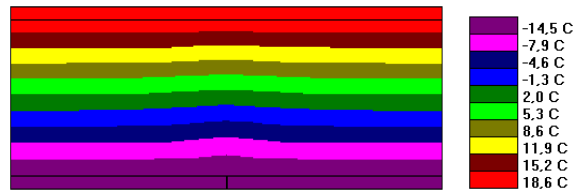
The results of the simulation show that the cracks in the covering of the lightweight construction filled with permeable thermal insulation lead to substantial changes in the temperature distribution and subsequently to the considerable increase in the heat loss. If the cracks are to be found on both sides of the construction opposite each other, the amount of $0,37 \text{ W}\cdot\text{m}^{-1}\cdot\text{K}^{-1}$ could be added under the presumption of the operating pressure difference of 10 Pa to the total heat loss for every 1 m of the crack length and for every 1 K of the operating temperature difference.



the pressure field



the air flow velocity field

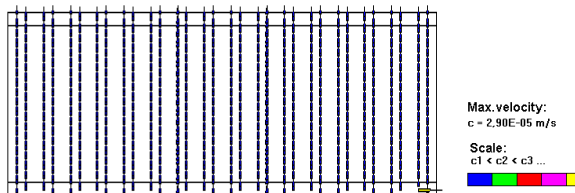


the temperature field

Fig. 6 The graphical presentation of the results for the construction with the crack in one plasterboard only



the pressure field

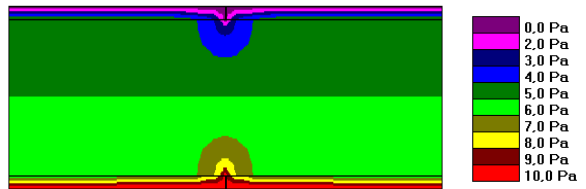


the air flow velocity field

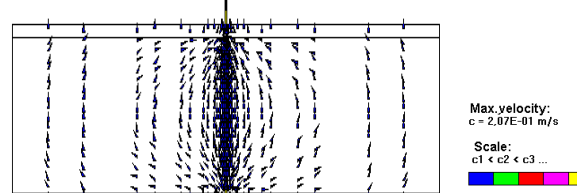


the temperature field

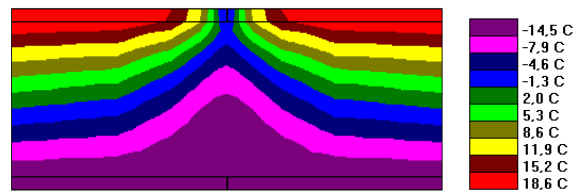
Fig. 5 The graphical presentation of the results for the tight construction



the pressure field



the air flow velocity field



the temperature field

Fig. 7 The graphical presentation of the results for the construction with the opposite cracks in both plasterboards

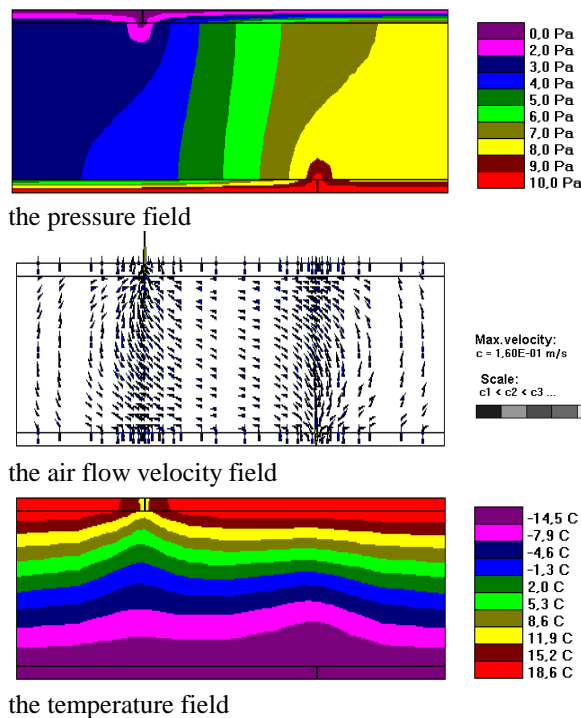


Fig. 8 The graphical presentation of the results for the construction with the cracks in both plasterboards in distance of 200 mm

CONCLUSIONS

The computer model „WIND“ could be used for the calculation of the temperature distribution in various types of building constructions. This work presents its application as a tool for the analysis of one typical lightweight wall construction.

The results of the numerical modelling show these major conclusions:

- The modern constructions containing the permeable thermal insulation from the mineral wool are very sensitive to the convective heat transfer.
- Any crack in the mineral wool covering could cause the air flow into the thermal insulation and subsequently the essential modifications in the temperature field.
- The result of such temperature distribution deformation is the considerable increase of the heat loss through the construction.

REFERENCES

Zienkiewicz, O.C., Taylor, R.L., „The Finite Element Method, Fourth edition“, McGraw-Hill, 1991.

Huebner, K.H., Thornton, E.A., „The Finite Element Method for Engineers, Second edition“, J. Wiley & Sons, 1982.

Jiranek, M., Svoboda, Z. „The Verification of Radon Protective Measures by Means of a Computer Model“, In: Building Simulation 97, The proceedings of the 5th International IBPSA Conference, Vol. II, pp. 165-172, Prague 1997.

Svoboda, Z., „The Numerical Solutions of the Combined Heat and Radon Transfer Caused by Diffusion and Convection“, PhD thesis, Prague 1997.

NOMENCLATURE

A	area of construction [m ²]
b	one half of the width of the crack [m]
c_a	thermal capacity of the air [1010 J.kg ⁻¹ .K ⁻¹]
h	size of an element in the velocity direction [m]
k	permeability of the porous medium [m ²]
k_a	„equivalent“ permeability of the air in the crack [m ²]
K_λ	conductance matrix
K_v	convective heat transport matrix
K_α	boundary conditions matrix
L	length of the crack in the direction of the air flow [m]
l	width associated with the U value [m]
l_v	length of the crack associated with the convective linear thermal transmittance [m]
N_i	interpolation functions vector
p	pressure of the air [Pa]
q_α	boundary conditions vector
T	temperature [K]
T_i	vector of unknown temperature values [K]
\bar{T}	known temperature at element boundary [K]
t_i	interior temperature [K]
t_e	exterior temperature [K]
U	U value, thermal transmittance coefficient [W.m ⁻² .K ⁻¹]
u	velocity component in the x axis direction

$ \mathbf{u} $	velocity vector magnitude
\vec{v}	velocity vector of air flow [m.s ⁻¹]
v	velocity component in the y axis direction
v_n	velocity component normal to the boundary
\bar{v}	mean velocity of the laminar air flow in the crack [m.s ⁻¹]
V	air flow rate into the interior through the construction [m ³ .s ⁻¹ .m ⁻²]
W_i	weighting functions vector
α	heat transfer coefficient [W.m ⁻² .K ⁻¹] The values of 8 W.m ⁻² .K ⁻¹ for internal surface and 23 W.m ⁻² .K ⁻¹ for external surface were used in the presented study.
α_c	convective heat transfer coefficient [Wm ⁻² K ⁻¹]
α_r	radiative heat transfer coefficient [W.m ⁻² .K ⁻¹]
Γ_e	boundary of a finite element
Φ	heat flow rate [W.m ⁻¹]
μ	viscosity of the air [1,7.10 ⁻⁵ Pa.s]
λ	thermal conductivity [W.m ⁻¹ .K ⁻¹]
Ω_e	area of a finite element
ρ_a	density of the air [1,2 kg.m ⁻³]
$\Psi_{v,\Delta p}$	convective linear thermal transmittance for given pressure difference [W.m ⁻¹ .K ⁻¹]
Δt	temperature difference [K]
ΔP	pressure difference between the inlet and the outlet of the crack [K]